Well log study and seismic survey of a coal-bed methane site: Alder Flats, Alberta

Jason McCrank, Han-xing Lu, Kevin W. Hall and Don C. Lawton

ABSTRACT

The seismic reflection characteristics of a coal-bed methane reservoir are studied with synthetic modeling and a seismic field survey. The reservoir consiste of two coal seams encountered at depths of 404 m and 414 m below surface. The coals are understood to be saturated with an aqueous phase. A simple rock physics model is assumed in order to investigate the AVO response of the existing wet coals and that of hypothetical "dry" coals. The model results show that the seismic reflectivities of the wet and dry coals are sufficiently distinct that the AVO response should discriminate between the two states of water saturation. In the summer of 2006, two 1C-2D seismic lines were acquired by the University of Calgary at the study site using an ENVI mini-vibe source. Although the source sweep was 10-200 Hz, the reflected energy had lesser bandwidth with a major peak in the amplitude spectrum at ~30 Hz and a lesser peak ~75 Hz. The signal to noise ratio diminishes above 100 Hz. Reflection continuity and frequency content improve by excluding near-offsets from the stack. Radial trace filtering is successfully used to remove linear noise from the shot gathers. Various methods of boosting amplitudes at higher frequencies (spectral whitening, surface-consistent deconvolution, Gabor deconvolution) improve data quality in the 0-100 Hz range. Although the signal bandwidth is limited and the target are thin, closely space beds, the coals are resolved as two distinct events in the migrated seismic section.

INTRODUCTION

At the commencement of coal-bed methane (CBM) production, methane is sorbed onto the coal matrix. The methane is de-sorbed from the matrix and then produced by reducing the pressure in the fracture space of the coals. However, in many cases, the water saturation of the coals is initially too high to allow economic quantities of methane to be produced. In these cases, the water is produced until the pressure in the reservoir is reduced to the point at which economic methane production ensues.

This paper investigates the seismic reflection response of water-saturated wet and de-watered dry coals. Petrophysical log data from a well near Alder Flats, Alberta in the Pembina Field was used to model the AVO response of a potential CBM producing coal reservoir. The coals belong to the Ardley Coals which are known to possess high inherent water saturation. The AVO response of the wet coals and that of hypothetical dry coals is modeled in order to determine if the response is sufficiently distinct to discriminate the two saturation conditions in a reflection seismic survey.

To further advance the study, two 1C-2D seismic lines were acquired by University of Calgary in June of 2006 near the study well.

PETROPHYSICAL LOGS

The edited density, compressional wave speed, shear wave speed, and gamma logs are shown in FIG. 1 for the study well. The statigraphy varies between units with high gamma log values (here referred to as shale) and units with lower gamma log readings (here referred to as sandstone, though they are not strictly "clean" and their exact lithology is unknown), and three coal seams at depths of 356 m, 404 m, and 414 metres. All identified geological picks are for the purpose of this report as illustrated in FIG. 1.

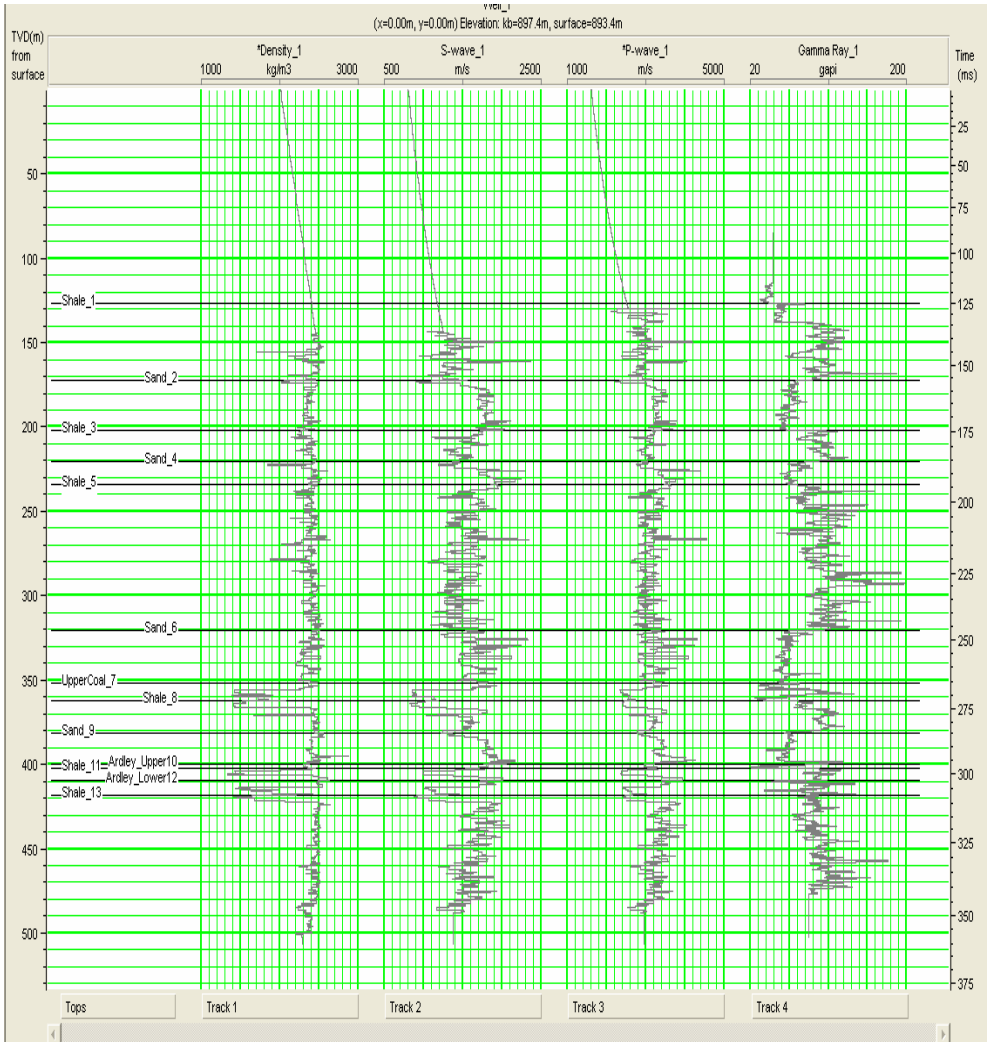

FIG. 1. Edited density, shear wave speed, compressional wave speed, and gamma logs for the injection well with formation tops.

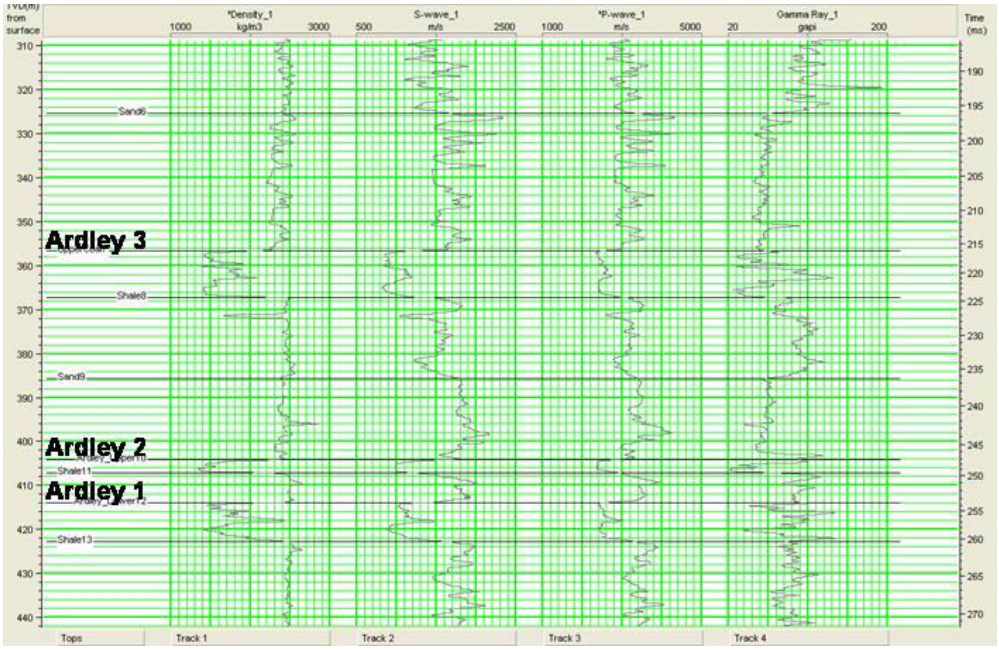

FIG. 2. Density, shear wave speed, compressional wave speed, and gamma logs for the study well showing details from the vicinity of the Ardley Coals. Three seams of the Ardley Coal Zone are identified. The lower two are studied as potential CBM producing seams.

The three coal seams are part of the Ardley Coal Zone, a sub-member of the Tertiary Scollard Formation, and are named here from deepest to shallowest as Ardley 1, Ardley 2, and Ardley 3 coals. The Ardley 1 and 2 seams have been identified for potential CBM production. FIG. 2 illustrates the logs in the vicinity of the target coals. Ardley 1 is at a depth of 414 metres and is approximately 9 m thick and Ardley 2 is at a depth of 404 m and is 4 metres thick. There is a non-coal stringer in middle the Ardley 1 seam. Both of the Ardley 1 and 2 seams are underlain by shales and Ardley 2 is overlain by sandstone.

PROPERTIES OF WET AND DRY COALS

Wet and dry coals are expected to have different elastic properties. Research by others (Richardson and Lawton, 2002), showed that Ardley Coals exhibit an approximate 26.9% reduction in P-wave speed and approximately 18% reduction in density when coals that are initially water saturated are completely dewatered in a laboratory setting.

Complete desiccation of coals is unlikely to occur in a reservoir environment. Additionally, as the water is removed from the coal cleats, methane gas will be released from the coal matrix and fill the cleats. As a result, the *in situ* rock properties are not expected to exactly mimic those observed in the laboratory environment. Richardson (2003) assumed a reduction of 10% in each of the P-wave speed and density to model dry coals. S-wave speed was assumed to be unaffected by the dewatering process. Table 1 lists the elastic properties of the Ardley Coal seams based on the averages from the well logs and the assumed changes in the properties if the coals were dry (Richardson, 2003).

Table 1. Average velocities and densities for the Ardley Coal seams.

Coal seam	Depth below surface (m)	Wet/Dry Coals	Average Density (kg/m3)	Average Vp (m/s)	Average Vs (m/s)	Vp/Vs
Ardley 2	404.4	Wet	1619	2498	1104	2.26
		Dry	1457	2248	1104	2.04
Ardley 1	414.1	Wet	1797	2567	1097	2.34
		Dry	1617	2310	1097	2.11

ZOEPPRITZ REFLECTION COEFFICIENTS

The Zoeppritz Explorer (CREWES) was used to investigate the PP and PS reflection coefficients as a function of incidence angle. FIG. 3a illustrates R_{pp} and R_{ps} for the top of Ardley 2 seam assuming average P-wave, S-wave, and density values from the well logs (i.e. wet coals). The Ardley 2 seam is overlain by a sandstone package. There is a significant gradient to both R_{pp} and R_{ps} over the incident angle range of 0° to 45°. FIG. 3b illustrates R_{pp} and R_{ps} for the top of Ardley 2 seam if the coals were dry (assuming the values from Table 1).

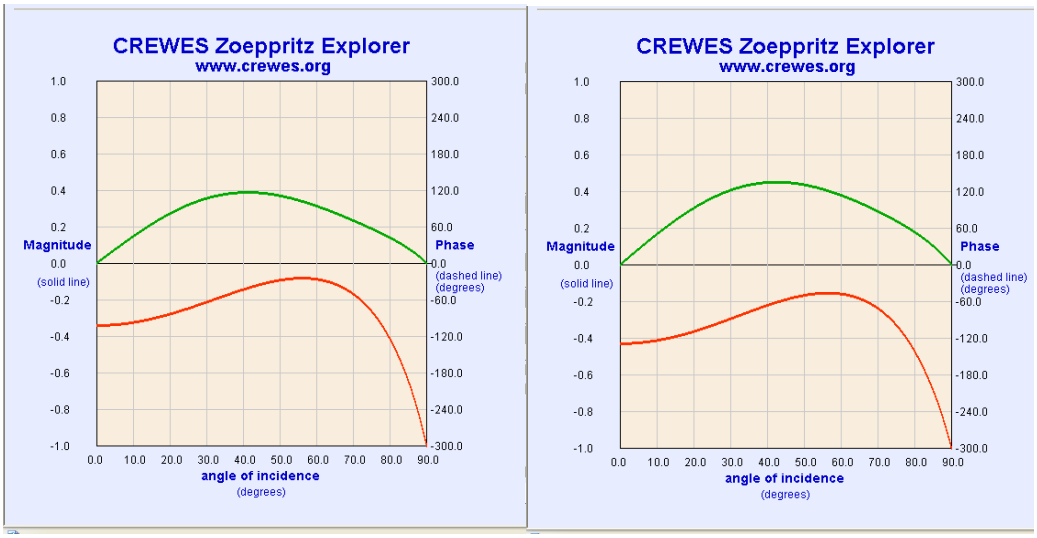

(a) (b)

FIG. 3. Reflection coefficients for PP (red) and PS (green) waves at the top of Ardley 2 seam. (a) wet coals, (b) dry coals.

Comparing Rpp for the wet and dry coals in the figures shows that the normal incidence reflection coefficient increases approximately 25% from the wet to dry case. Analytically calculating the normal incidence Rpp using the acoustic impedance contrast for the two cases shows an increase of 26.1% from the wet to the dry coals.

The Rpp gradient is not notably different between the wet and dry coals. However, comparing Rps for the two cases, the gradient is slightly greater for the dry coals than the wet coals.

FIG. 4 shows the Rpp and Rps for the base of Ardley 2 seam which is underlain by a shaley zone. Again, the normal incidence Rpp is higher for the dry coals, but the Rpp gradient does not show a great difference. The Rps gradient is steeper for dry coals than for wet coals.

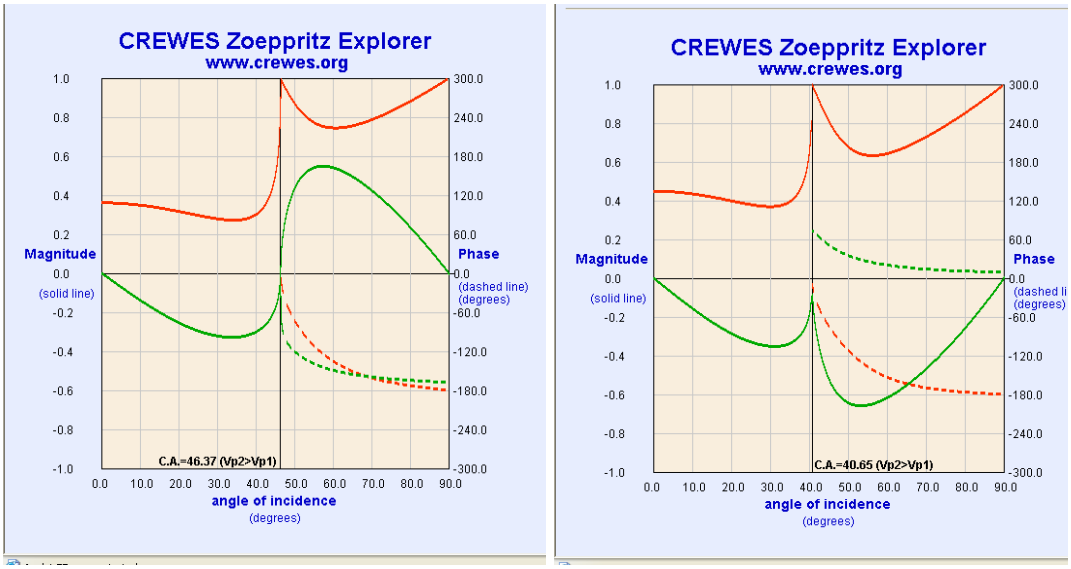

(a) (b)

FIG. 4. Reflection coefficients for PP (red) and PS (green) waves at the base of Ardley 2 seam. The solid line indicates the magnitude and the dashed line indicates the phase. (a) wet coals, (b) dry coals.

SYNTHETIC MODELING WITH SYNGRAM

The Syngram program developed by the CREWES research group was used to model the AVO gathers for surface seismic surveys. The model neglected the effects of transmission loss, spherical divergence, attenuation, and multiples. The model results used the SEG display standard for polarity. All wavelets modeled were assumed to be zero phase.

Figure 5 shows the PP AVO gather with a 90 Hz Ricker wavelet. NMO has been removed and the display has been zoomed around the zone of interest. Other wavelets were modeled; however, a 90 Hz Ricker wavelet appeared to have a reasonable correlation with the field data from Alder Flats. FIG. 6 shows the PP synthetic generated by adjusting the density and P-wave logs in the Ardley Coal zones to reflect a 10% reduction corresponding to dry coals. Note, however, that the shale stringer that appears in Ardley 1 is not affected by the changes in elastic properties, so the density and P-wave speed were not reduced by 10% in this 1 metre zone.

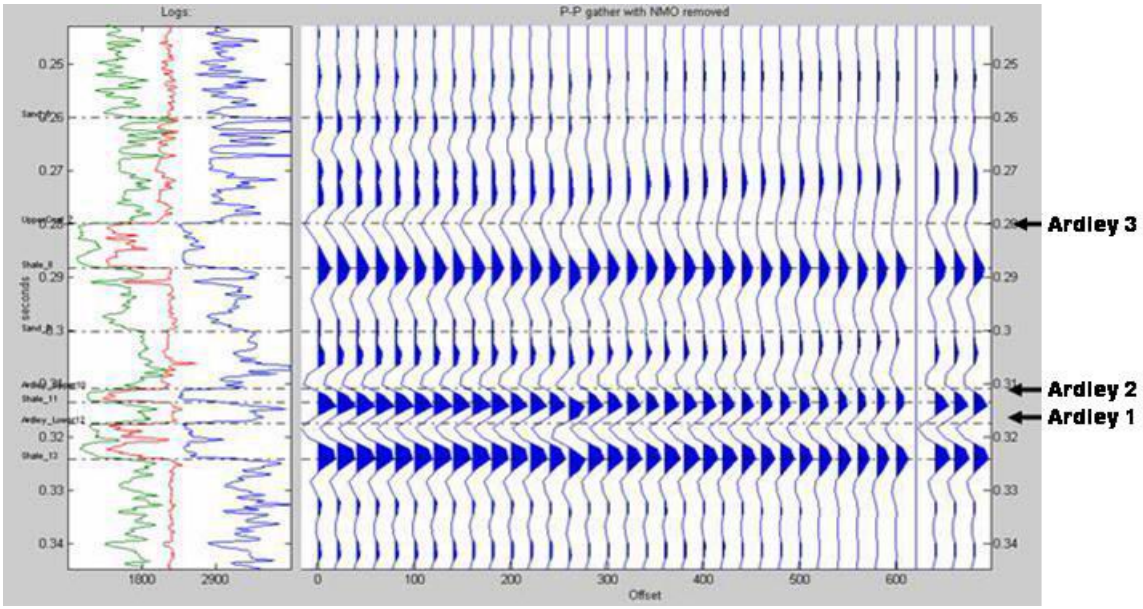

Reflection type	PP	Logs/rock properties	Wet coals
Max offset/depth ratio	2	Wavelet	Ricker 90Hz
Receiver type	Vertical geophone	Receiver response	Total motion
Maximum offset	600 m	Amplitude scale	1.5

Figure 5. PP gather – Ricker 90 Hz

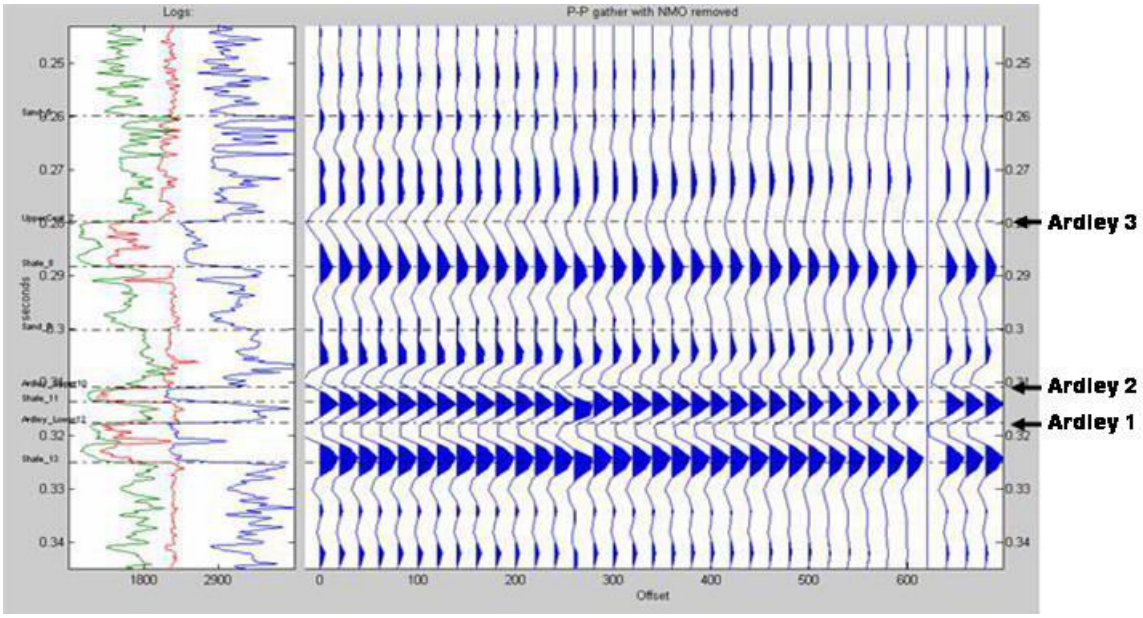

Reflection type	PP	Logs/rock properties	Dry coals
Max offset/depth ratio	2	Wavelet	Ricker 90Hz
Receiver type	Vertical geophone	Receiver response	Total motion
Maximum offset	600 m	Amplitude scale	1.5

FIG. 6. PP gather – 10 % reduction in density and P-wave speed in coals

For comparison, FIG. 7 shows a PP synthetic for a maximum offset of 1000 m. Though the AVO effect is more pronounced with the greater maximum offset in the PP gather, adequate gradient should be achieved with an offset of 600 metres. Also, for comparison, FIG. 7 incorporates a 60 Hz Ricker wavelet. Ardley 2 and Ardley 1 are not well resolved as separate events with the 60 Hz Ricker wavelet.

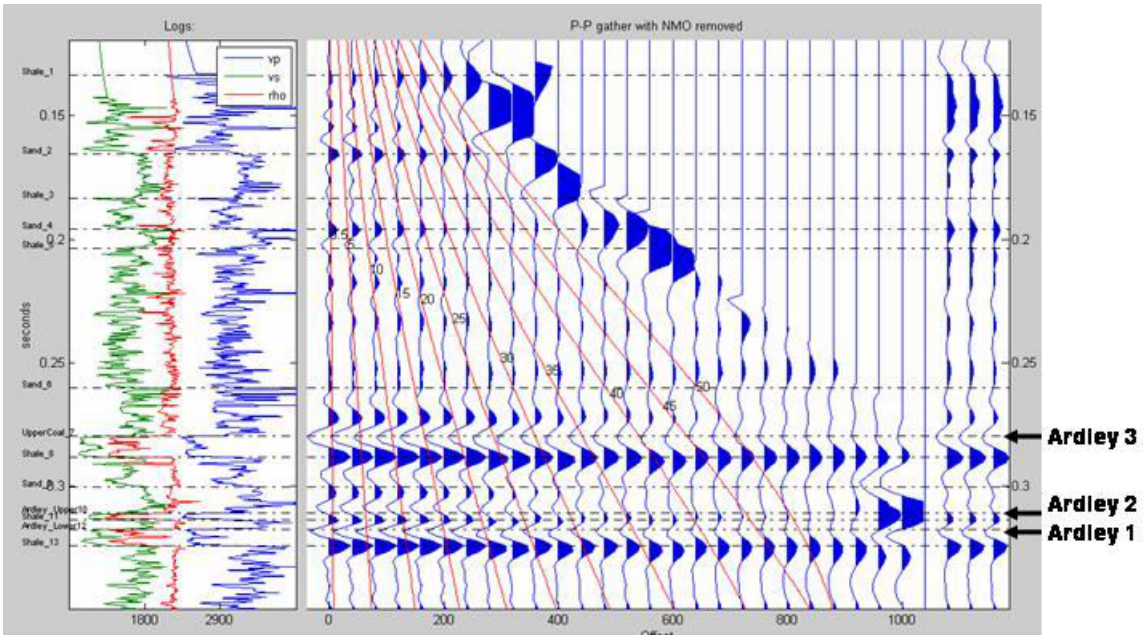

Reflection type	PP	Logs/rock properties	Wet
Max offset/depth ratio	2	Wavelet	Ricker 60Hz
Receiver type	Vertical geophone	Receiver response	Total motion
Maximum offset	1000 m		

FIG. 7. PP gather – 1000 m maximum offset, angles of incidence and 60Hz Ricker wavelet

AVO MODELING

The Hampson-Russell Software (HRS) AVO package was used to further investigate the AVO response of the coals. FIG. 8 illustrates the PP AVO gather and the variation of the amplitude for events at 308 ms and 314 ms. These events correspond to the base of Ardley 2 seam and the top of Ardley 1 seam which should be good indicators of the AVO effect of the coals. The model uses a 60 Hz Ricker wavelet.

FIG. 9 shows the AVO gradient and intercept from the dry coal's PP synthetic seismogram. Again, the density and the P-wave speed have been reduced by 10%. The graph shows the variation of amplitude for the same two events at 308 ms and 314 ms corresponding to the base of Ardley 2 and the top of Ardley 1, respectively. Differences in the normal incidence amplitude and the AVO gradient can be seen by comparing FIG. 8 and FIG. 9.

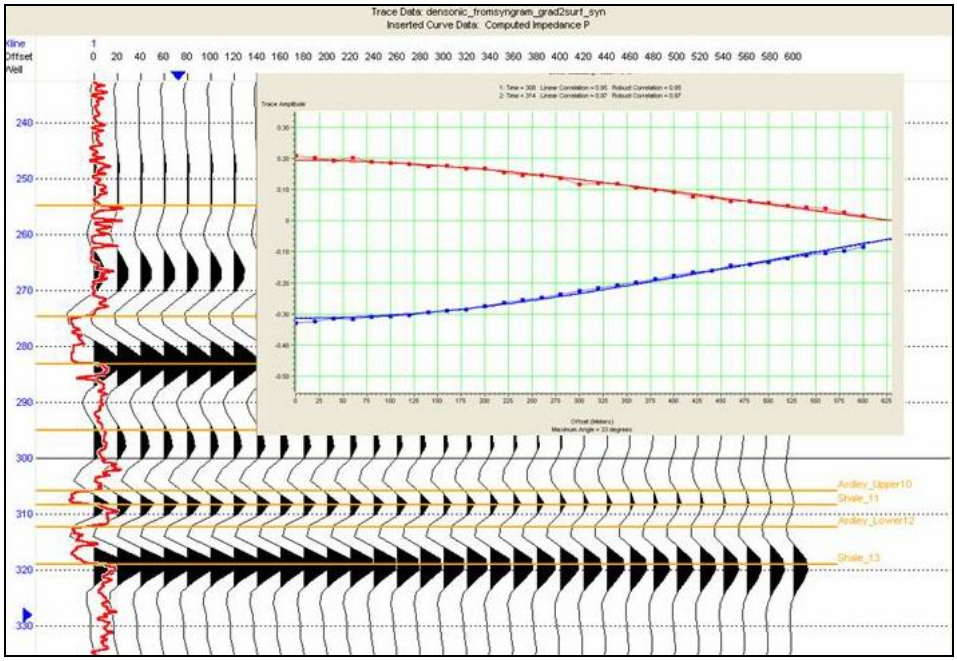

FIG. 8. The AVO gradient and intercept for the wet coals case. The inset shows the AVO intercept/gradient at the base of Ardley 2 (red) and at the top of Ardley 1 (blue). The background is the AVO PP synthetic. The log is acoustic impedance.

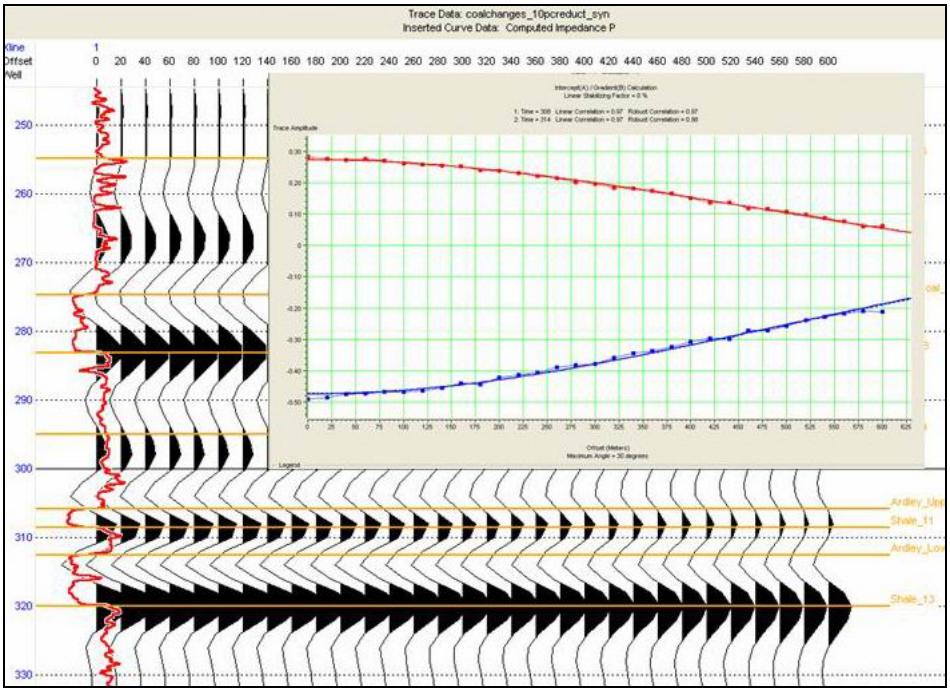

FIG. 9. The AVO gradient and intercept for the dewatered coals case. The inset in the figure on the right shows the AVO intercept/gradient at the bottom of Ardley 2 (red) and at the top of Ardley 1 (blue). The background is the AVO PP synthetic. The log is acoustic impedance.

A "wedge" model was generated for the Ardley 1 seam to test the sensitivity of the AVO response to the thickness of the coal seam. The PP results modeled with a 60 Hz Ricker wavelet are illustrated in FIG. 10. The seam was varied in thickness from 4 m to 15 m in one metre increments. The top of the seam is held at a constant depth, while the thickness of the coal is stretched. The thickening seam retains its original log character which is merely stretched.

FIG. 10 shows that a maximum in the amplitude of Ardley 1 event occurs when the seam thickness is 10 m. This is the tuning thickness of Ardley 1 seam. The top and the bottom of the coal seam will therefore not be well resolved with a 60 Hz Ricker wavelet if the seam is less than 10 m thick.

Analytically, for coals with a P-wave speed of 2567 m/s (average Ardley 1 wave speed), the dominant wavelength of a 60 Hz wavelet will be 42.8 m. The Widess criterion for the limit of resolution is $\lambda/8 = 5.35$ m (Widess, 1973). However, using the $\lambda/8$ criterion as the limit of resolution assumes ideal circumstances. A more conservative estimate of the limit of resolution is $\lambda/4$. With the $\lambda/4$ criterion, the limit of resolution of Ardley 1 is 10.7 m.

In the study well, the Ardley 1 seam has a thickness of approximately 9 m. Therefore, a wavelet with significant band width higher than 60 Hz may be required to resolve the top and bottom of the Ardley 1 seam. An 80 Hz wavelet with a dominant wavelength of 32.1 m in Ardley 1 seam would have a limit of resolution of 8.0 m. Likewise, the Ardley 2 seam, that is approximately 4 m in thickness, would require a wavelet with a dominant frequency of 160 Hz to resolve the top and bottom of the seam (using the $\lambda/4$ criterion).

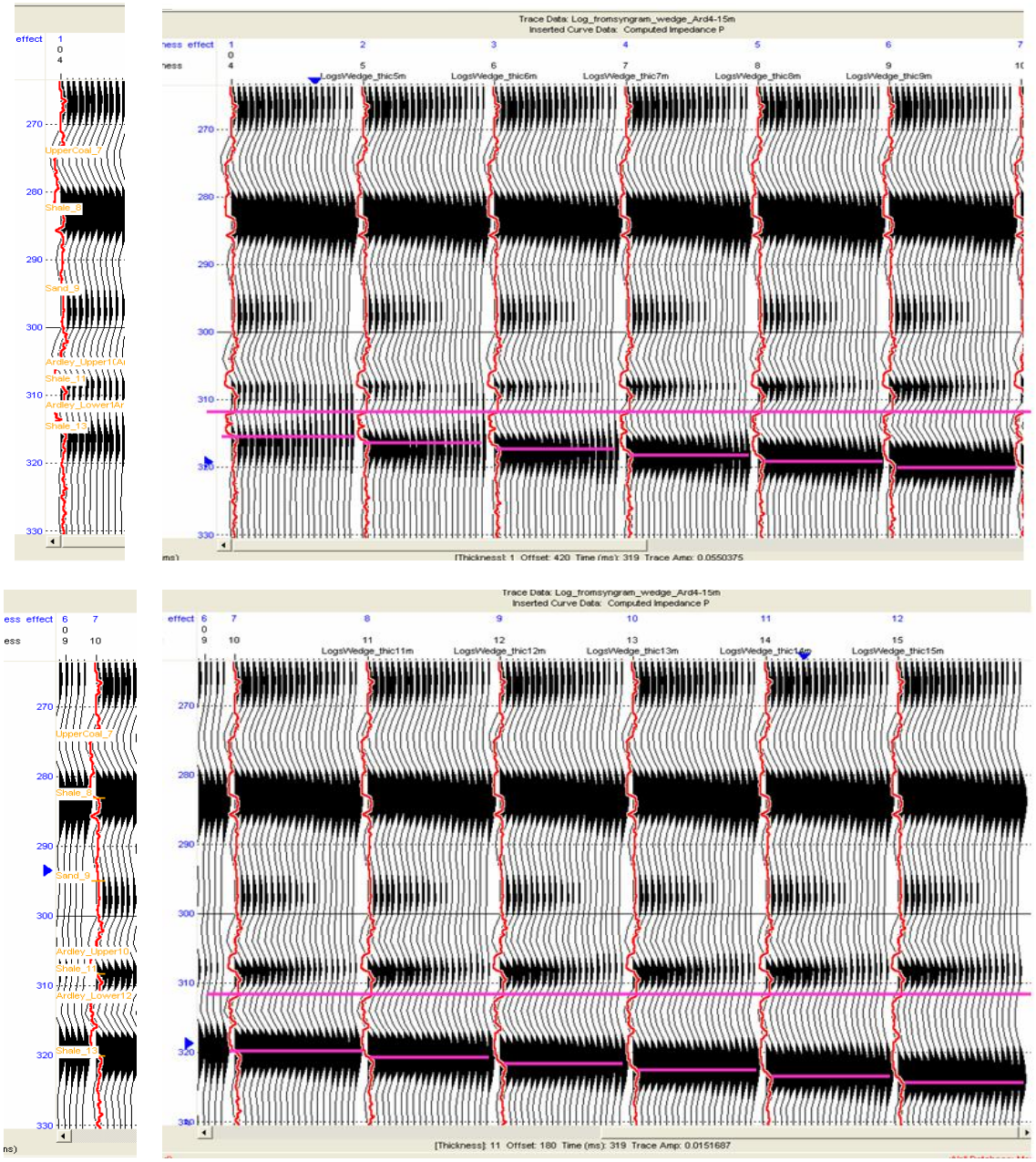

FIG. 10. A wedge model of Ardley 1 seam. There are 12 AVO gathers. Each corresponds to a 1 m thickening of Ardley 1 seam from a thickness of 4 m to a thickness of 15 m. The purple lines delineate the wedge of Ardley 1. The actual seam is close to 9 m thick and corresponds to the right most gather in the top set. The red lines are the acoustic impedance logs. The track on the left shows the formation tops at a wedge thickness of 4 m for the top set and 10 m for the bottom set. The model uses a 60 Hz Ricker wavelet.

Small variances in the thickness of the coals will effect the travel time through the seam and therefore change the reflected wave form. The effect on the AVO response of varying the Ardley 1 seam from 8 m to 10 m thick was investigated (though not shown).

The effect was found to be secondary in comparison to the difference in the AVO response of wet/dry coals.

JUNE 2006 FIELD SURVEY

Two 1C-2D seismic lines were acquired by University of Calgary in June of 2006 at the study location near Alder Flats, Alberta. One line was oriented approximately north to south and the second was oriented east to west. The N-S line is closest to the study well. These lines were acquired to test the Department of Geology and Geophysics' new ENVI mini-vibe source and ARAM recording system, and site characterization in order to help design future time-lapse surveys.

ACQUISITION

The Alder Flats 2006 survey consists of two 1C-2D lines with a total line length of about 4 km. The data were acquired using single vertical-component marsh phones every 5 m. Nominal source interval was a 10 m interval for the North-South (N-S) line and a 30 m interval for the East-West (E-W) line (FIG. 11, Table 2). Four sweeps per source point were diversity stacked and correlated in the field.

Table 2. Acquisition parameters.

Source	EnviroVibe
Sweep frequency	10-200 Hz
Vertical stack	Diversity Stack
Source interval	10 m for N-S line, 30 m for E-W line; 4 sweeps per VP
Receivers	SM-24 Marsh phone (10 Hz dominant)
Receiver interval	5 m for N-S and E-W lines

a)

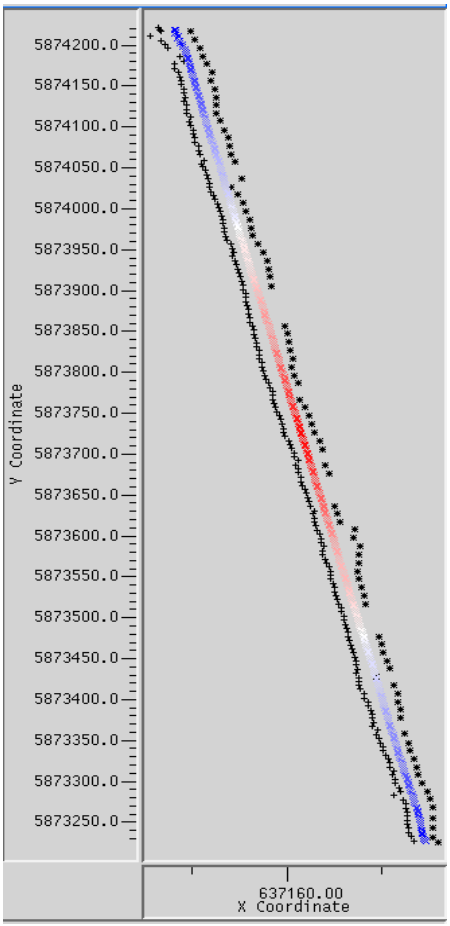

b)

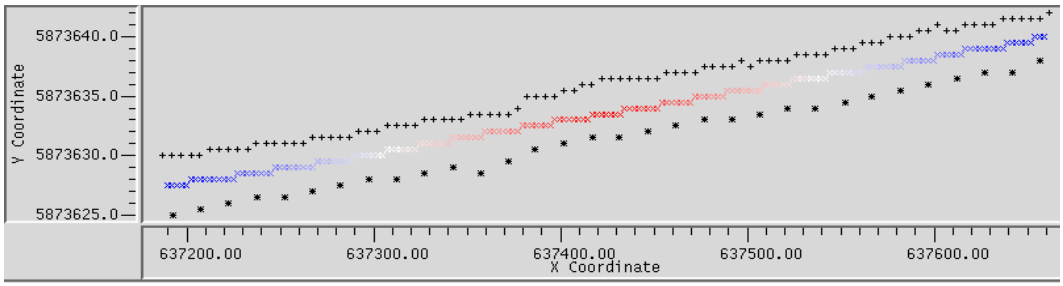

FIG. 11. Survey geometry (modified from ProMAX). Source locations (right, Figure 2a; bottom, Figure 2b) from GPS antenna mounted above EnviroVibe base-plate. Geophone locations were individually surveyed. CDP fold is shown in colour.

PROCESSING

The raw shot gathers contain fairly strong source noise (FIG. 12), typically more prominent on the N-S line. The E-W line has a better signal/noise (S/N) ratio than the N-S line. This is illustrated in FIG. 12. Comparing the reflectivity in the blue boxes, the

peak at 100 Hz in the amplitude spectrum is at 11 dB down on the E-W line as compared to 17 dB down on the N-S line. It is not known exactly why the shot records show this S/N difference. Possible explanations are that the receiver locations in the ditch alongside the N-S road allowance were lower and significantly wetter than the field in which the E-W line was acquired or source coupling issues.

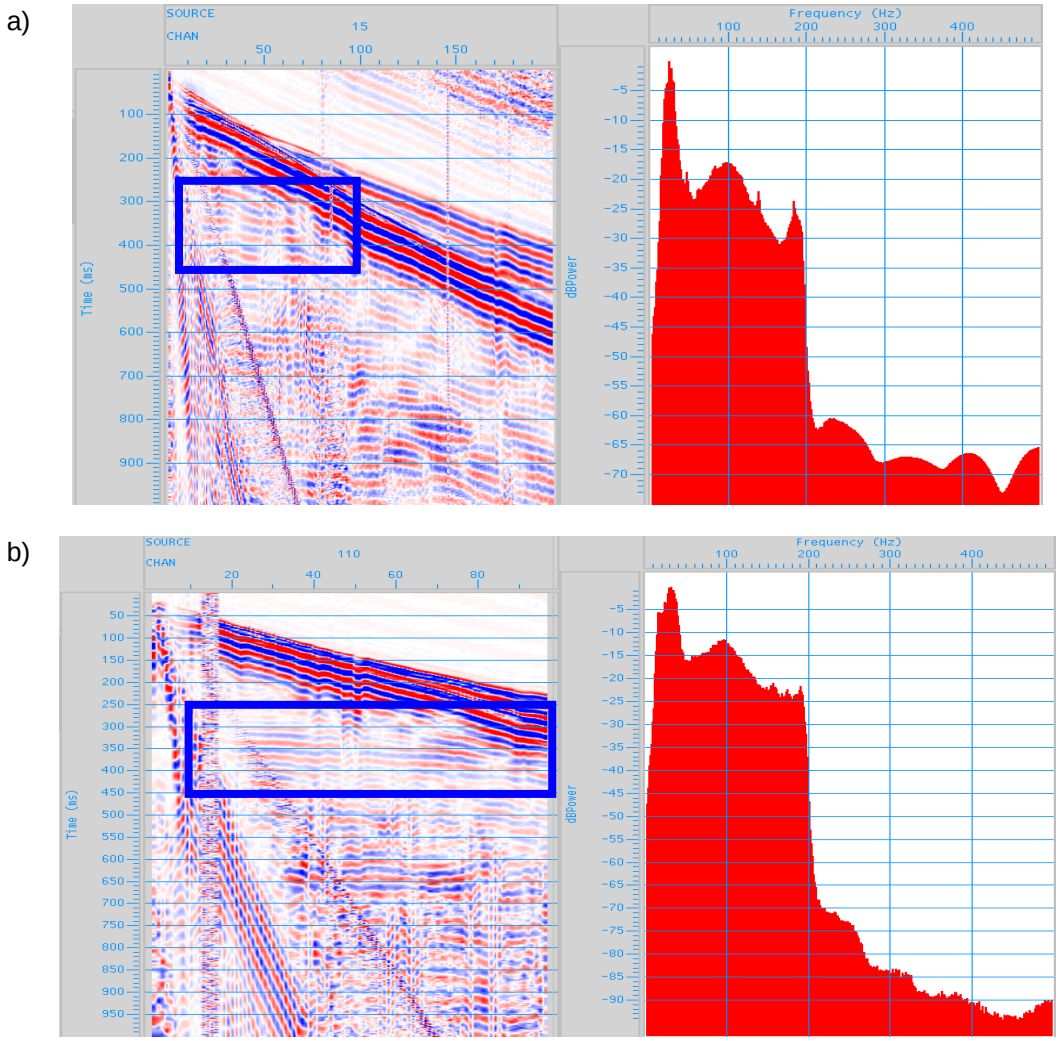

FIG. 12. Raw shot gathers and associated amplitude spectra for: (a) N-S line, and (b) E-W line. Blue rectangles are 100 traces x 200 ms.

Source-receiver offset range tests

FIG. 13 through FIG. 17 show a series of migrated sections for the N-S line, with source-receiver offsets limited to 0-1000 m, 60-1000 m, 200-1000 m and 400-1000 m. As near-offsets are progressively excluded, reflections in the target zone become more continuous (cf. blue boxes in the figures). The same effect is also observed deeper in the section (cf. red boxes in the figures). While an improvement is seen, some of these near-offsets need to be retained, or shallow reflections disappear from the section (e.g. FIG. 17).

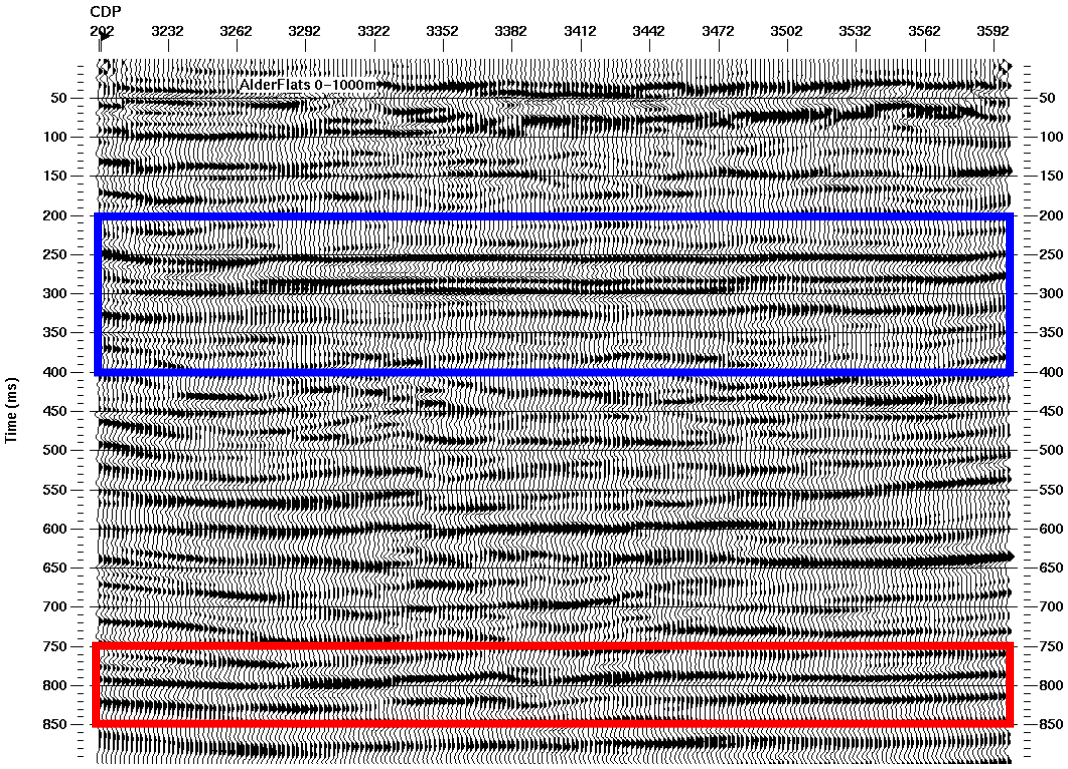

FIG. 13. N-S Line: Migrated section for 0-1000 m source-receiver offsets.

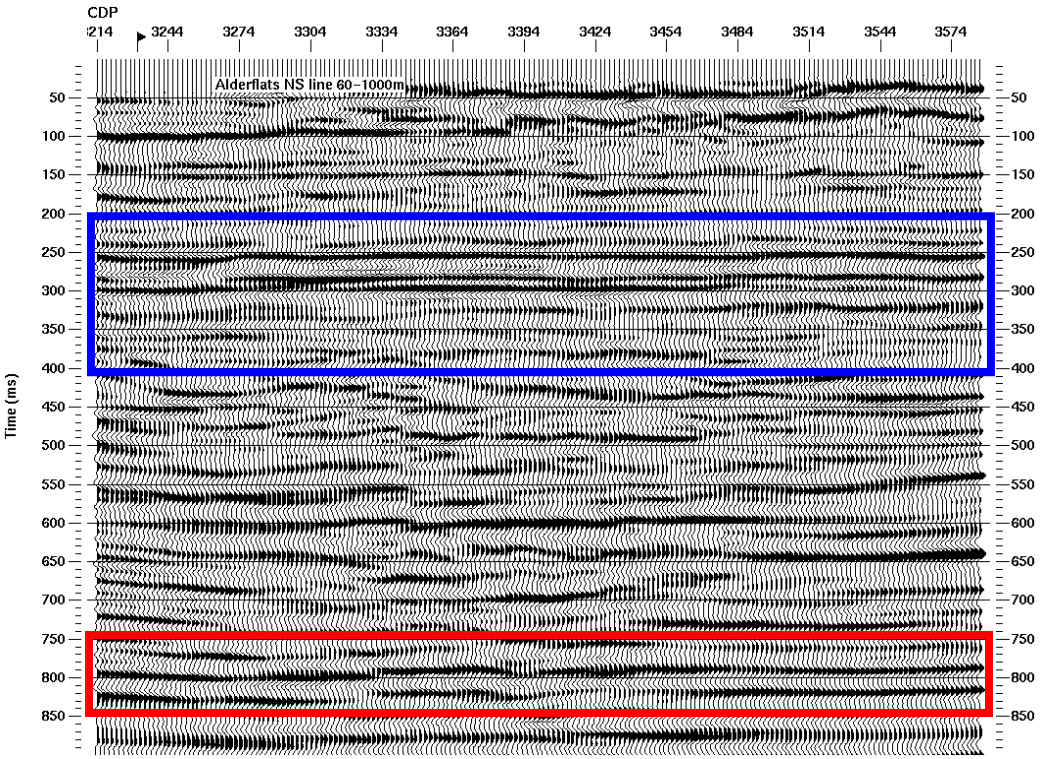

FIG. 14. N-S Line: Migrated section for 60-1000 m source-receiver offsets.

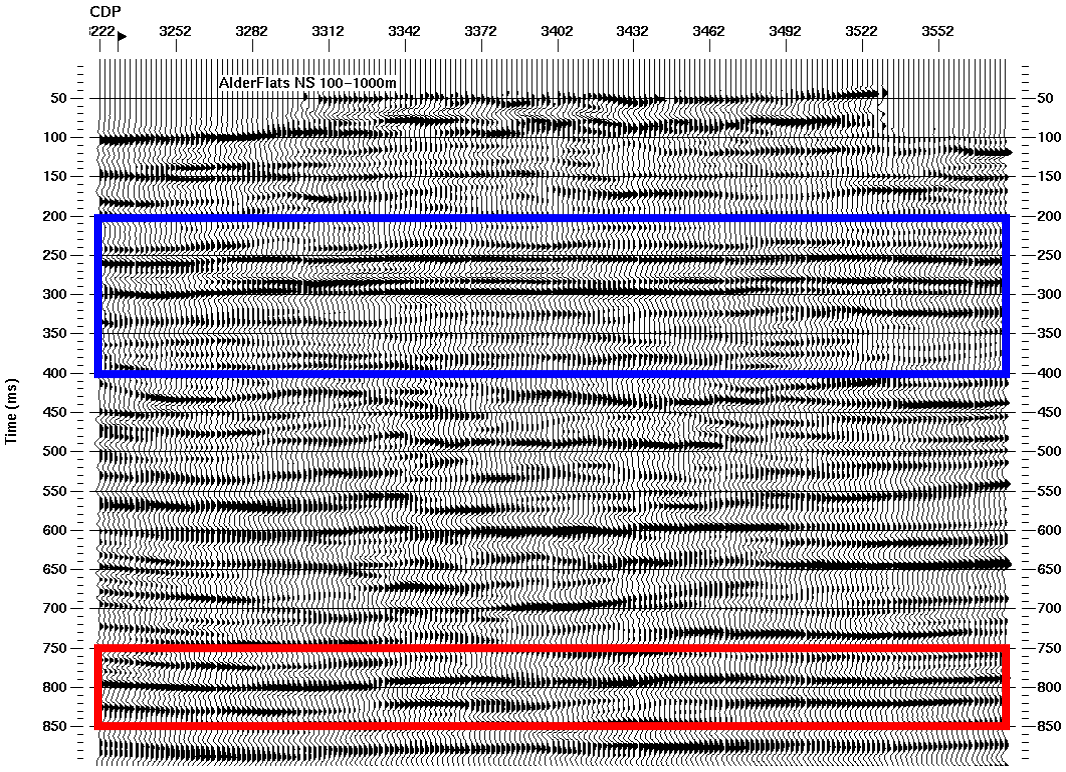

FIG. 15. N-S Line: Migrated section for 100-1000 m source-receiver offsets.

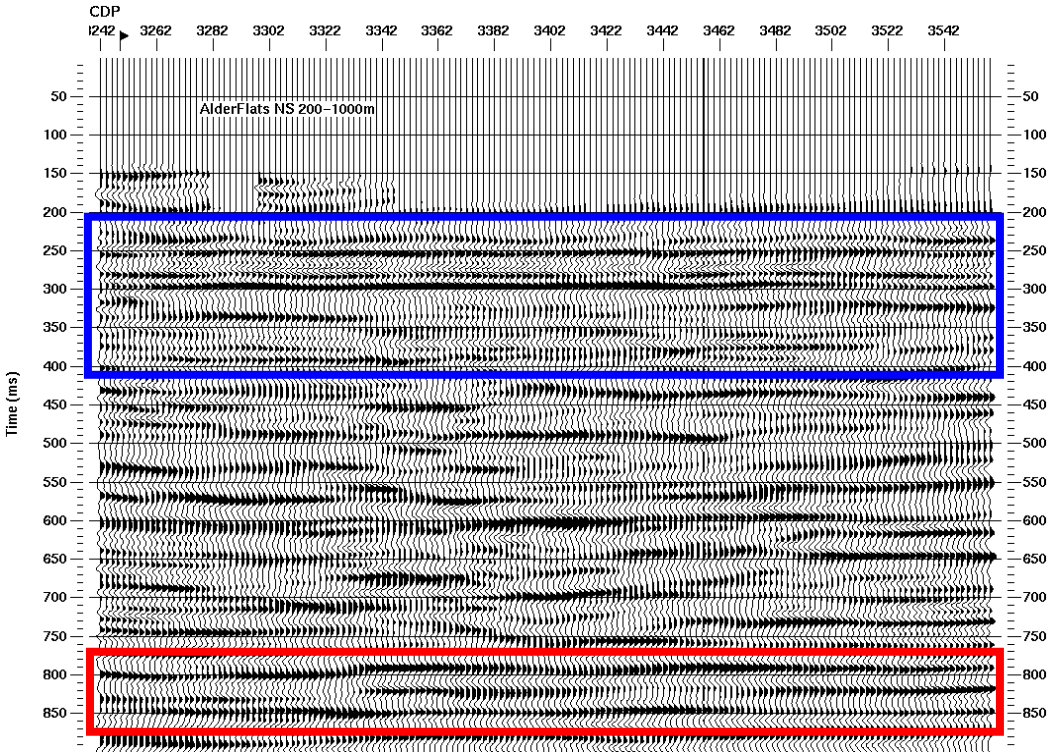

FIG. 16. N-S Line: Migrated section for 200-1000 m source-receiver offsets.

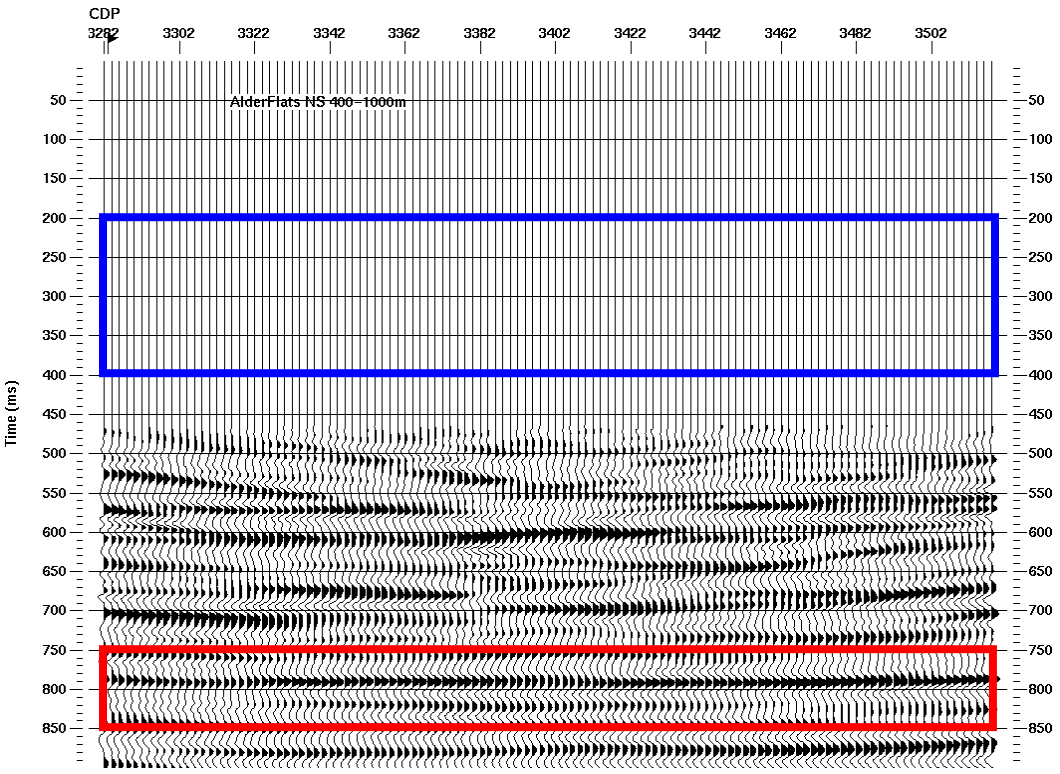

FIG. 17. N-S Line: Migrated section for 400-1000 m source-receiver offsets.

Standard processing results

Since the maximum sweep frequency was 200 Hz, any signal seen in the section above 200 Hz will be noise. For these data, spectral whitening above 100 Hz appears to increase noise amplitudes only, and does not significantly affect the stacked results (not shown). Both lines were processed using a standard CREWES processing flow (Table 3), and the results are shown in FIG. 18 and FIG. 19. These sections have had spectral whitening applied over 12-100 Hz, followed by a bandpass filter over the same frequency range. Based on the results shown in FIG. 13 through FIG. 17, the source-receiver offset range was limited to 60-1000 m. With identical processing, reflections near the target on the E-W line (blue rectangle, FIG. 18) are more continuous and contain higher frequencies than on the N-S line (FIG. 19).

Table 3. Vertical processing flow, modified from Lu and Margrave (1998).

TRACE EDIT
TRUE AMPLITUDE RECOVERY
SURFACE CONSISTENT DECONVOLUTION
TIME VARIANT SPECTRAL WHITENING
ELEVATION AND REFRACTION STATIC CORRECTIONS
VELOCITY ANALYSIS
RESIDUAL SURFACE CONSISTENT STATICS
NORMAL MOVEOUT
TRIM STATICS
FRONT END MUTING
CDP STACK
TIME VARIANT SPECTRAL WHITENING
TRACE EQUALIZATION
F-X DECONVOLUTION
PHASE-SHIFT MIGRATION
FOR TRACE DISPLAY:
TRACE EQUALIZATION
BANDPASS FILTER
TIME VARIANT SCALING

Amplitude spectra for the migrated sections are shown in FIG. 20. FIG. 20a and FIG. 20b show the N-S line with and without spectral whitening. There is a noticeable improvement in the section with spectral whitening, but it should be mentioned that this is not an appropriate processing step if AVO analysis is planned. FIG. 20c shows the E-W line with spectral whitening for comparison. There is a notch in the spectra at about 57 Hz on both lines, which is more pronounced on the E-W line (15 dB down, as compared to 10 dB down for the N-S line; FIG. 20 b and c).

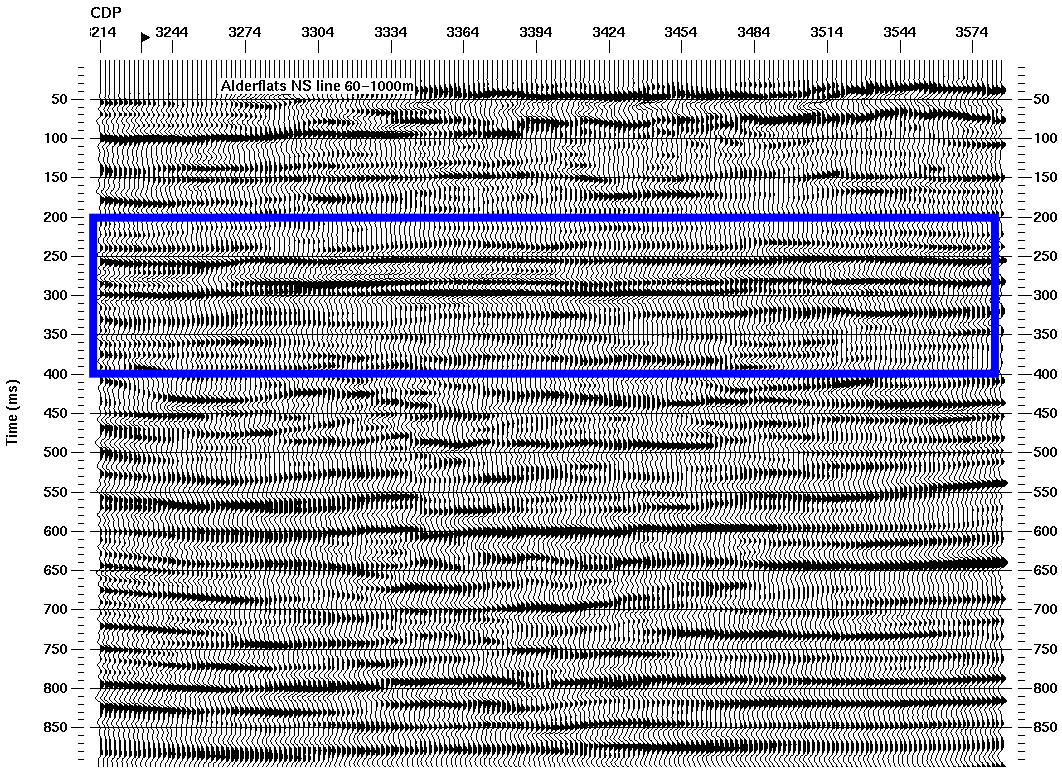

FIG. 18. N-S line; Migrated section obtained from conventional processing.

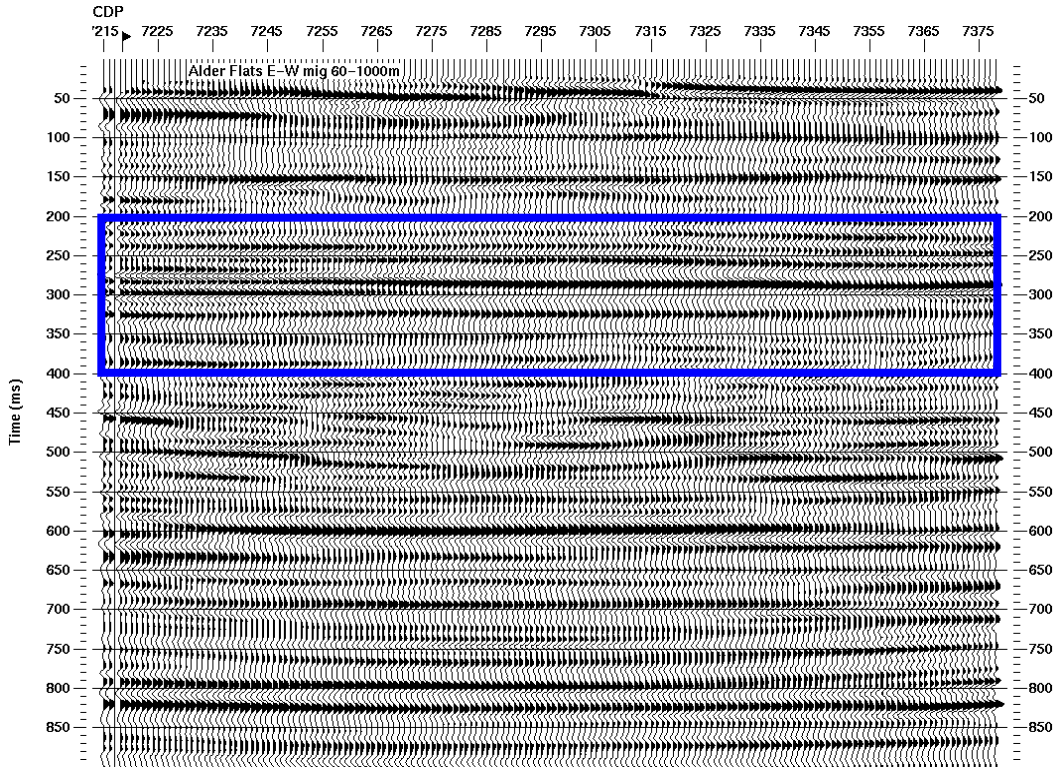

FIG. 19. E-W line; Migrated section obtained from conventional processing. Note that horizontal scale is not the same as for FIG. 13 through FIG. 17.

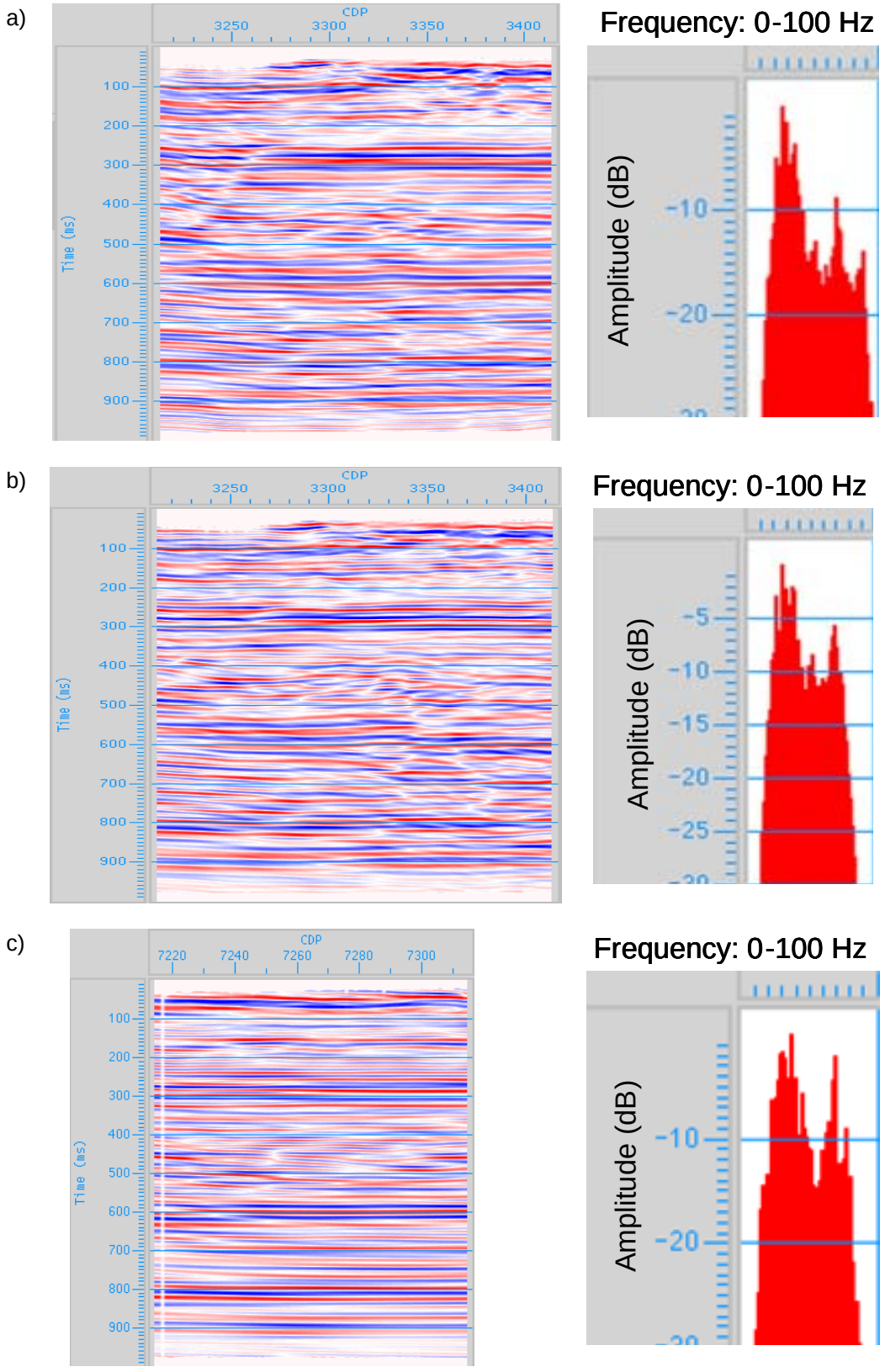

FIG. 20. Migrated sections and amplitude spectra: (a) N-S line with no spectral whitening, (b) N-S line with 12-100 Hz spectral whitening (cf. FIG. 18), and (c) E-W line with 12-100 Hz spectral whitening (cf. FIG. 19).

Other processing results

In order to remove linear noise such as source noise and direct arrivals, seven passes of radial trace filtering (Henley, 1999) were applied. Subtraction of modeled linear noise has improved data quality and does not truncate shallow reflections, unlike top-muting and excluding near-offsets (FIG. 21).

After radial filtering, Gabor deconvolution was applied to boost high frequency amplitudes in a time-varying way (FIG. 22; Margrave et al., 2002). As was the case for spectral-whitening, amplitudes above about 75 Hz appear to be noise only. FIG. 23 shows the same gather as FIG. 22, after a 10-15-100-120 Hz bandpass filter. If traces in the shot gather are misaligned, radial filtering can create artifacts (FIG. 23; blue rectangle). Fortunately, these will stack out, even without further processing.

FIG. 24 and FIG. 25 compare the migrated sections for the N-S line using conventional processing and a processing flow incorporating radial filtering and Gabor deconvolution.

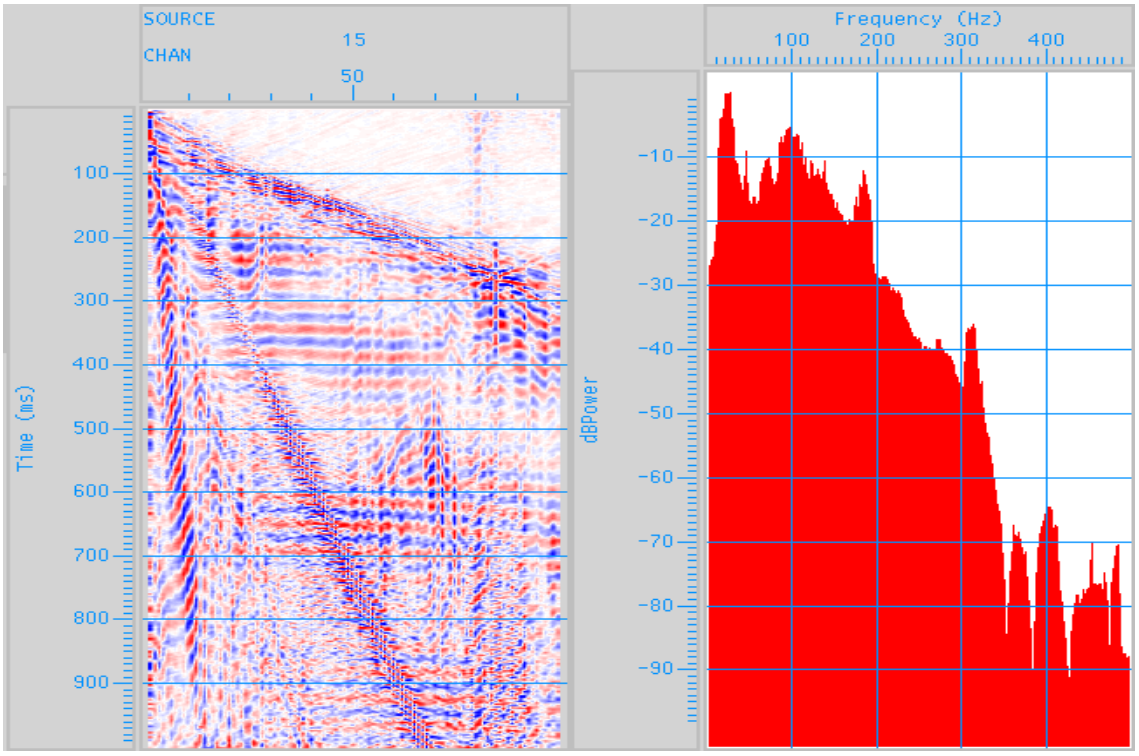

FIG. 21. N-S line: Shot gather after seven-pass radial trace filter.

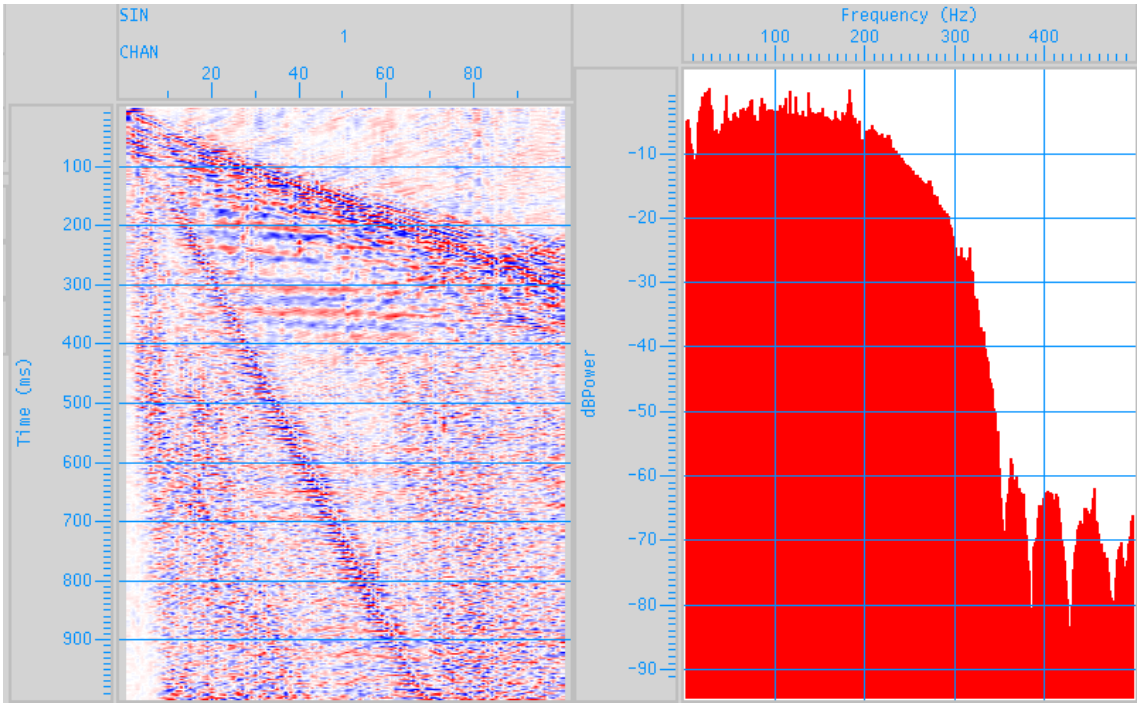

FIG. 22. N-S line: Shot gather after seven-pass radial trace filter and Gabor deconvolution.

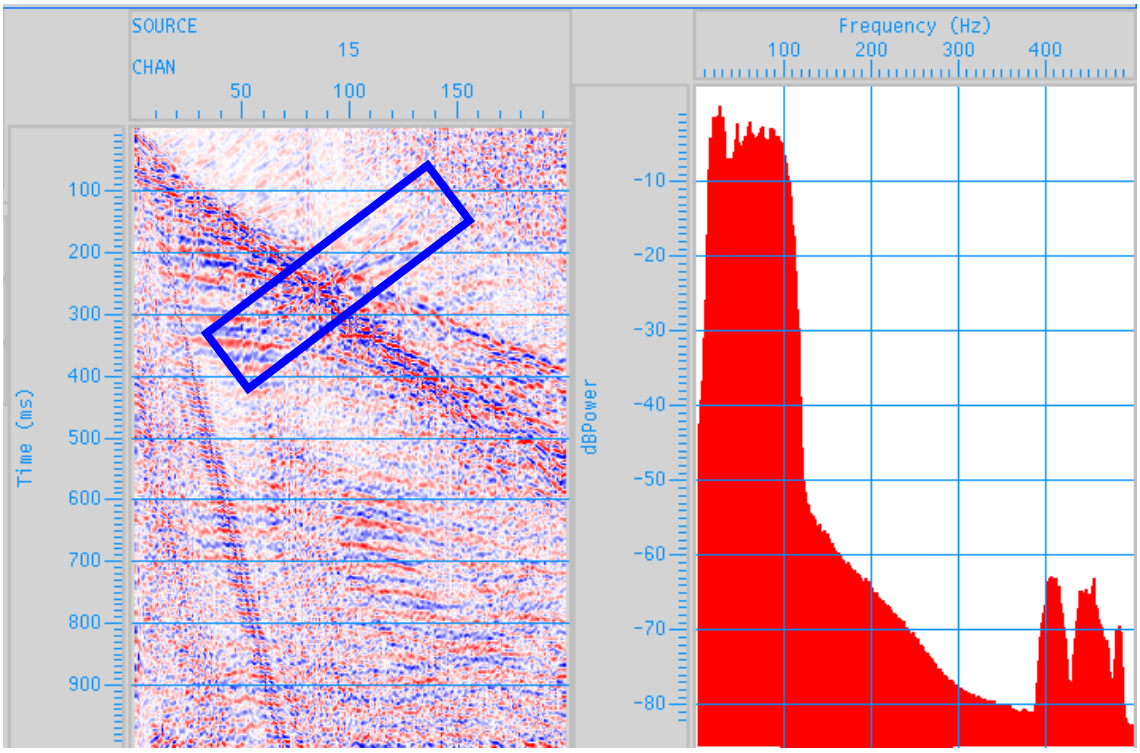

FIG. 23. N-S line: Shot gather after seven-pass radial trace filter, Gabor deconvolution, and 10-15-100-120 Hz bandpass filter. Note linear artifact due to a misaligned trace in raw shot gather (blue rectangle).

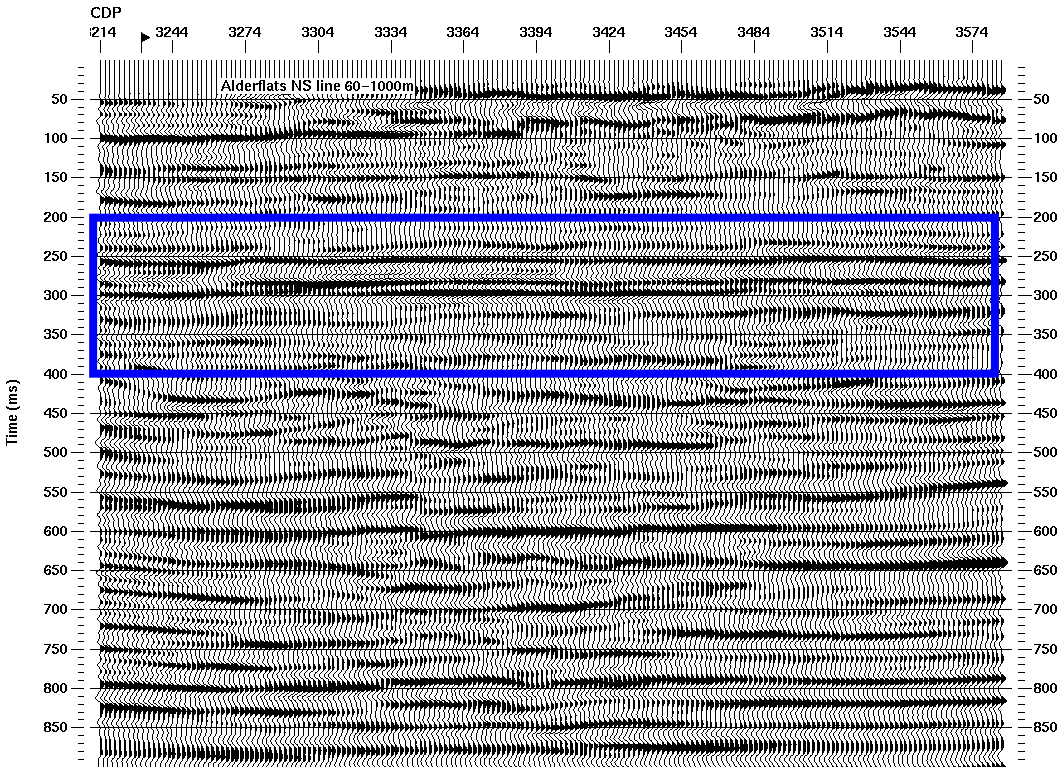

FIG. 24. N-S line; Migrated section obtained from conventional processing (FIG. 18).

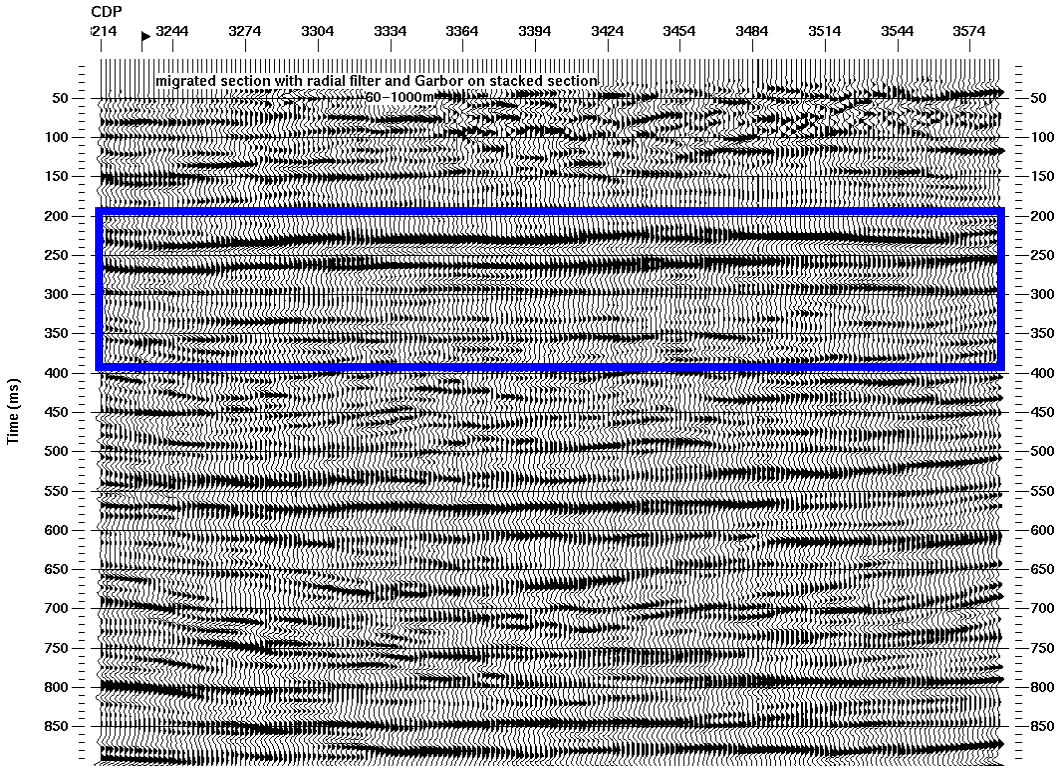

FIG. 25. N-S line; Migrated section after radial filtering and Gabor deconvolution.

SURVEY INTERPRETATION

FIG. 26 shows the tie between the synthetic seismogram generated with a 90Hz Ricker wavelet and the migrated data from the N-S line. The study well is approximately 100 metres east of the survey line. The Ardley 1 and Ardley 2 are resolved as separate events. The black peaks correspond to the base of the coals.

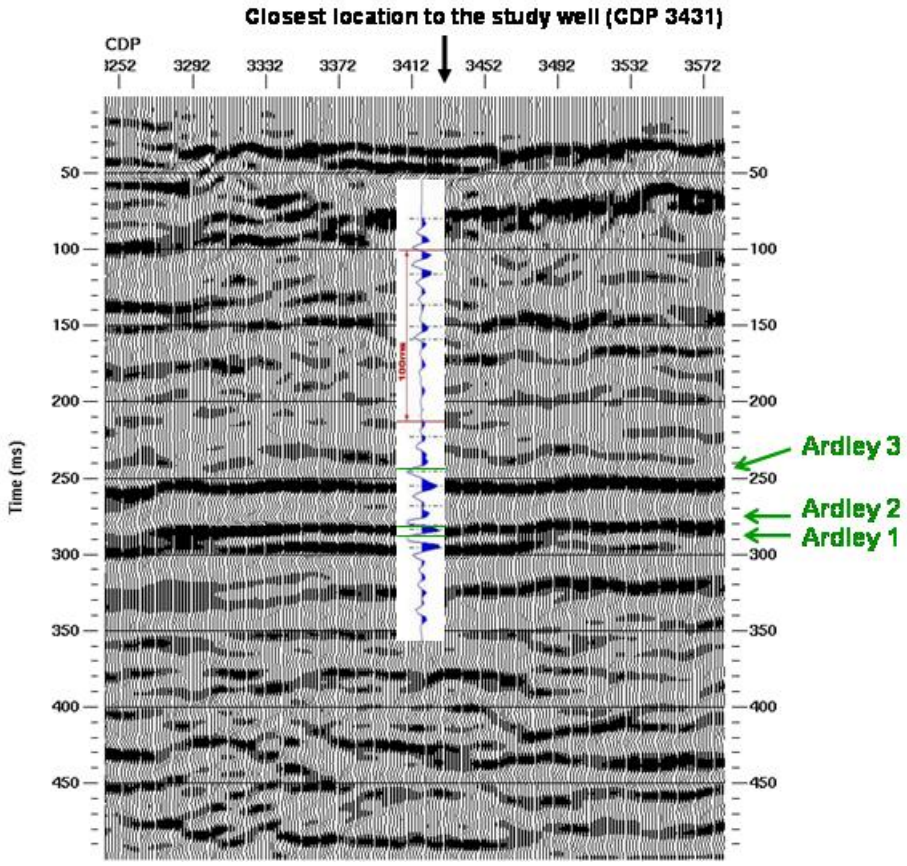

FIG. 26. Ardley Flats migrated data (conventional processing) N-S line with tie to a stretched 90 Hz Ricker wavelet synthetic.

CONCLUSIONS

The model results show that the AVO seismic reflectivities of the wet and dry coals are sufficiently distinct to resolve the two states of water saturation. The effect of slight variations in coal seam thickness will have a secondary effect on the AVO response as compared to the distinction in the AVO response of wet or dry coals. However, because thin-bed tuning effects are expected with the coal seams, the modeling shows that bandwidth above 90 Hz will be required to resolve the two seams as separate seismic events.

In the field survey, although the source sweep was 10-200 Hz, the reflected energy had lesser bandwidth with a major peak in the amplitude spectrum at ~30 Hz and a lesser peak ~75 Hz. The signal to noise ratio diminishes above 100 Hz.

Reflection continuity and frequency content are improved in the seismic section by excluding near-offsets from the stack. Radial trace filtering successfully removes linear noise from the shot gathers. Various methods of boosting amplitudes at higher frequencies (spectral whitening, surface-consistent deconvolution, Gabor deconvolution) improve data quality in the 0-100 Hz range.

Although the signal bandwidth is limited, the target coals are resolved as two distinct events in the migrated N-S seismic section that is closest to the study well.

ACKNOWLEDGEMENTS

The authors would like to thank Malcolm Bertram, Henry Bland, Eric Gallant, Fuju Chen, Kelley Classen, Nathan Dahlby and Aqsha for field support. We would also like to thank all CREWES sponsors, especially Landmark Graphics and Hampson Russell for the use of ProMAX, gli3d, and AVO. Funding for the field program was supported by NSERC.

REFERENCES

Henley, D. C., 1999, Radial trace computational algorithms at CREWES: CREWES Research Report, **11**.

Lu, H., and Margrave, G. F., 1998, Reprocessing the Blackfoot 3C-3D seismic data: CREWES Research Report, **10**.

Margrave, G. F., Henley, D. C., Lamoureux, M. P., Iliescu, V. I., and Grossman, J. P., 2002, An update on Gabor deconvolution: CREWES Research Report, **14**.

Richardson, Sarah E., and Lawton, Don C., 2002. Time-lapse seismic imaging of enhanced coalbed methane production: a numerical modeling study: CREWES Research Report, **14**.

Richardson, Sarah E., 2003, Seismic applications in coalbed methane, M.Sc. thesis, University of Calgary.

Widess, M., 1973, How thin is a thin bed?, Geophysics, **38**, 1176-1254.